

CALCULATING BPM COEFFICIENTS WITH GREEN'S RECIPROCATION THEOREM*

S. H. Kim[†], Advanced Photon Source, Argonne National Laboratory, Argonne, IL

Abstract

Green's reciprocity theorem was applied to four-button beam position monitors (BPMs) for the calculation of BPM coefficients. Induced potentials on the buttons in geometries of a small-gap and a circular beam chamber were calculated as examples.

1 INTRODUCTION

An induced current, due to a highly relativistic charged particle beam on the chamber wall, will have the same longitudinal intensity modulation as the charged particle beam. When the wavelength of the beam intensity modulation is large compared with the dimensions of the button electrodes, which are used as BPMs, the calculation of the induced currents on the buttons may be simplified as a 2-D electrostatic problem. Green's reciprocity theorem (or reciprocity relation for electrostatic problems) [1] is applied to four-button BPMs in this paper. BPM coefficients are calculated by conformal mappings for geometries of a small-gap and a circular beam chamber.

2 GREEN'S RECIPROCATION THEOREM

First, we consider that a set of n charges q_1, q_2, \dots, q_n on n conductors will give rise to potentials V_1, V_2, \dots, V_n on the conductors. The potential V_m on conductor m is dependent on all q_i except q_m . If a different set of charges $q_{p1}, q_{p2}, \dots, q_{pn}$ gives rise to potentials $V_{p1}, V_{p2}, \dots, V_{pn}$, then Green's reciprocity theorem states that

$$\sum_{i=1}^n q_i V_{pi} = \sum_{i=1}^n q_{pi} V_i. \quad (1)$$

Equation (1) may be applied to analyze a system of four-button BPMs as shown in the cross section of a beam chamber in Fig. 1(a). At first the beam chamber, as well as the BPM buttons, are assumed to be grounded. If we place a point charge q_o at a beam position (x_o, y_o) , then induced charges $q_1, q_2, q_3,$ and q_4 will appear on the four buttons. (We assume that the potential at the beam position is V_s .) We then remove the charges from the beam position and the buttons in order to have a new set of charges and potential. This time, if we apply a potential of $+V_p$ to all four buttons (and at the same time we assume a charge distribution of $q_{p1}, q_{p2}, q_{p3},$ and q_{p4} on the four buttons), a potential we call V_{ps} will be induced at the beam position. These two sets of charge/potential distributions are summarized in Table 1. Then, from Eq. (1) we have the

relation, $q_o V_{ps} + (q_1 + q_2 + q_3 + q_4) V_p = 0$, or

$$\frac{Q_s}{(-q_o)} = \frac{V_{ps}}{V_p}, \quad (Q_s = q_1 + q_2 + q_3 + q_4). \quad (2)$$

We may also apply the potential V_p on the buttons in two different configurations besides the above case for all $+V_p$. By setting the upper two buttons to $+V_p$ and the lower two buttons to $-V_p$, the potential at (x_o, y_o) will be called V_{py} . Similarly, by setting the right two buttons to $+V_p$ and the left two buttons to $-V_p$, the potential at (x_o, y_o) will be called V_{px} . Then, from Eq. (1) we have

$$\frac{Q_y}{(-q_o)} = \frac{V_{py}}{V_p}, \quad (Q_y = q_1 + q_2 - q_3 - q_4), \quad (3)$$

$$\frac{Q_x}{(-q_o)} = \frac{V_{px}}{V_p}, \quad (Q_x = q_1 - q_2 - q_3 + q_4). \quad (4)$$

Equations (2) - (4) imply that induced charges $Q_s, Q_y,$ and Q_x , corresponding to the sum, vertical, and horizontal signals for q_o at (x_o, y_o) , are proportional to the induced potentials $V_{ps}, V_{py},$ and V_{px} at (x_o, y_o) , respectively. When the position of q_o changes, $Q_s, Q_y,$ and Q_x change due to the redistribution of the induced charges on the buttons. This is equivalent to having different induced potentials at the new beam position.

Except for a few cases of simple chamber geometry, derivations of analytical expressions for the induced charges on the buttons are limited. When finite-element modeling must be used to calculate induced charges on the buttons, one mesh geometry is required for each beam position (x_o, y_o) , making it almost impossible to have a complete set of calculations in the BPMs plane. Instead, when Eqs. (2) - (4) are used after applying Green's reciprocity theorem, the three induced potentials $V_{ps}, V_{py},$ and V_{px} may be calculated by applying potentials $+V_p$ or $-V_p$ on the buttons using only one set of mesh geometry, which simplifies the calculation significantly.

Table 1: Charge/Potential Distributions (b: button)

	(x_o, y_o)	b 1	b 2	b 3	b 4
Charge (q_i)	q_o	q_1	q_2	q_3	q_4
Voltage (V_i)	V_s	0	0	0	0
Charge (q_{pi})	0	q_{p1}	q_{p2}	q_{p3}	q_{p4}
Voltage (V_{pi})	V_{ps}	V_p	V_p	V_p	V_p

3 OPTIMIZED CONFIGURATION IN A SMALL-GAP BEAM CHAMBER

Figure 1 shows the conformal mapping of the inner region of a "small-gap" beam chamber in the z -plane into the upper half-plane of the w -plane under the

* Work supported by the U.S. Department of Energy, Office of Basic Energy Sciences, under Contract No. W-31-109-ENG-38.

[†]shkim@aps.anl.gov

transformation $w = i\exp(pz)$, where $p = \pi/2h$ and h is the half-gap of the chamber. We assume that the chamber width is much larger than its gap height. (A width-to-height ratio larger than 5 gives sufficiently accurate results when compared with calculations using Green's function method for rectangular chambers.) The charge $q_o(z_o)$ in the z -plane is then located at w_o in the w -plane.

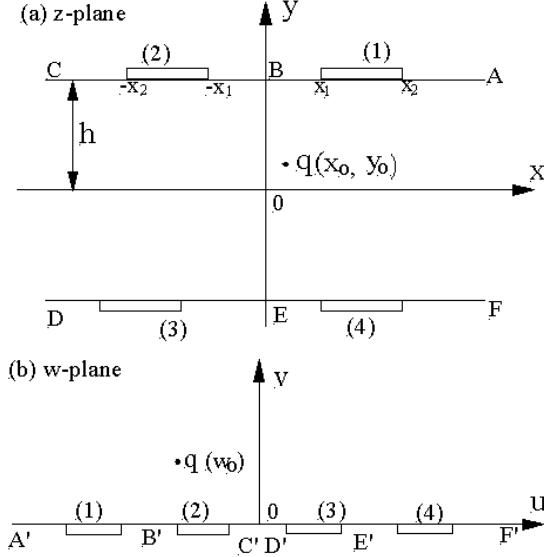


Figure 1: Conformal mapping of a small-gap beam chamber from (a) z -plane to (b) w -plane for a relatively large width-to-height aspect ratio of the chamber by $w = i\exp(\pi z/2h)$.

For this relatively simple geometry, when a potential of $+V_p$ or $-V_p$ is applied on the buttons, the induced potentials V_{ps} , V_{py} , and V_{px} at the beam position may be calculated in the w -plane. First, assuming that the beam chamber is grounded, the induced potential at the beam position $V(x_o, y_o)$ due to potential V_p on one button may be calculated from the Poisson's formula for the upper half-plane:

$$V(x_o, y_o) = \frac{1}{\pi} \int \frac{v_o V(u) du}{v_o^2 + (u_o - u)^2} = -\frac{V_p}{\pi} \tan^{-1} \left(\frac{u_o - u}{v_o} \right) \Bigg|_{u=u_1}^{u=u_2}, \quad (5)$$

where $u_o = -\exp(px_o) \sin py_o$, $v_o = \exp(px_o) \cos py_o$, and u_1 and u_2 are the button locations corresponding to x_1 and x_2 in Fig. 1(a). Then, for four buttons located symmetrically with respect to the x - and y -axes, V_{ps} and V_{py} , were calculated from Eqs. (2), (3), and (5):

$$V_{ps}(x_o, y_o) = \frac{V_p}{\pi} \left[\tan^{-1} \left\{ \frac{\sinh p(x - x_o)}{\cos py_o} \right\} + \tan^{-1} \left\{ \frac{\sinh p(x + x_o)}{\cos py_o} \right\} \right]_{x_1}^{x_2}, \quad (6)$$

$$V_{py}(x_o, y_o) = \frac{V_p}{\pi} \left[\tan^{-1} \left\{ \frac{\exp[2p(x - x_o)] + \cos 2py_o}{\sin 2py_o} \right\} - \tan^{-1} \left\{ \frac{\exp[2p(x + x_o)] + \cos 2py_o}{\sin 2py_o} \right\} \right]_{x_1}^{x_2}. \quad (7)$$

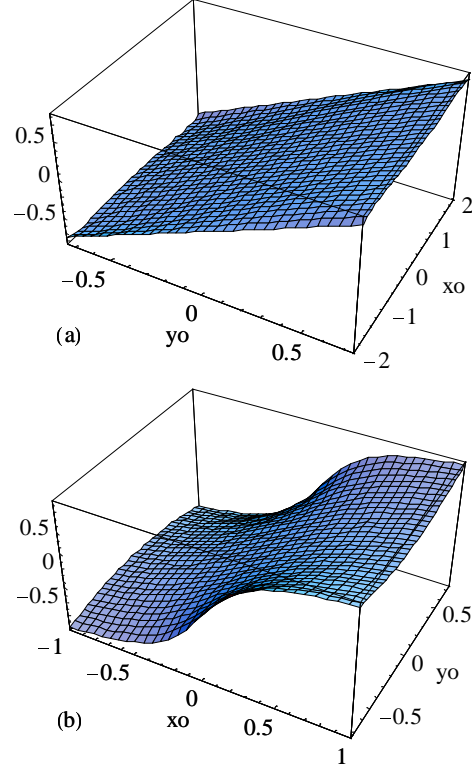


Figure 2: 3-D plots of (a) normalized vertical (V_{py}/V_{ps}) and (b) normalized horizontal (V_{px}/V_{ps}) signals in x_o/h - y_o/h plane for the optimized configuration in a small-gap beam chamber.

Figure 2 shows 3-D plots of the normalized vertical and horizontal signals, V_{py}/V_{ps} and V_{px}/V_{ps} , in the plane of normalized beam position $(x_o/h, y_o/h)$. The 3-D plots were calculated for the case of $x_1 = 0$ and $x_2 = 2h$, which is the optimized BPM configuration in a small-gap beam chamber [2]. For $|x_o/h| < 2$, the vertical signal shows excellent linearity with respect to the normalized vertical position. The horizontal signal, on the other hand, is rather nonlinear compared with the vertical one, for $|x_o/h| > 0.5$.

4 CIRCULAR BEAM CHAMBER

Four-button BPMs in a circular beam chamber of radius a in the z -plane are mapped into the w -plane in Fig. 3 under the transformation $w = i(a+z)/(a-z)$. The buttons are located symmetrically with respect to the x - and y -axes of the chamber. By summing up the induced potential from the four buttons, the potential for the sum signal $V_{ps}(x_o, y_o)$ due to potential V_p may be calculated from Eqs. (2) and (5):

$$V_{ps}(x_o, y_o) = -\frac{V_p}{\pi} \left[\tan^{-1} \left\{ \frac{u_o - \xi(\theta)}{v_o} \right\} \right]_{\theta_1}^{\theta_2} + \tan^{-1} \left\{ \frac{u_o - \xi(\theta)}{v_o} \right\} \Big|_{\pi-\theta_2}^{\pi-\theta_1} + \tan^{-1} \left\{ \frac{u_o - \xi(\theta)}{v_o} \right\} \Big|_{\pi+\theta_1}^{\pi+\theta_2} + \tan^{-1} \left\{ \frac{u_o - \xi(\theta)}{v_o} \right\} \Big|_{2\pi-\theta_2}^{2\pi-\theta_1} \right], \quad (8)$$

where $u_o = -2y_o / [(1-x_o)^2 + y_o^2]$,

$v_o = (1-x_o^2 - y_o^2) / [(1-x_o)^2 + y_o^2]$,

$\xi(\theta) = -\sin\theta(1-\cos\theta)$, $\theta_1 = \theta_p - \Delta\theta/2$, $\theta_2 = \theta_p + \Delta\theta/2$, and z is normalized to the chamber radius a .

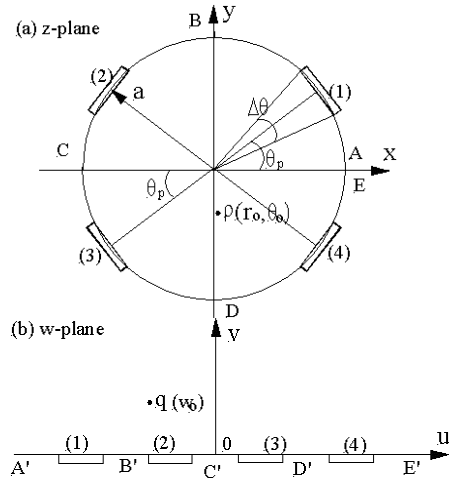


Figure 3: Conformal mapping of a circular chamber from (a) z -plane to (b) w -plane by $w = i(a+z)/(a-z)$. The buttons are located symmetrically with respect to the x - and y -axes in the z -plane.

The induced potential $V_{py}(x_o, y_o)$ and $V_{px}(x_o, y_o)$ for the vertical and horizontal signals may be obtained with minus signs in the third and fourth terms, and with minus signs in the second and third terms, respectively, in Eq. (8). In Fig. 4, (a) and (b) are 3-D plots of V_{py} and V_{py}/V_{ps} for four-button BPMs in the plane of radius r_o/a and angle θ_o . Before the normalization, both V_{py} and V_{ps} for $r_o/a > 0.5$ and near $\theta_o = \pi/2$ have relatively small values. This suggests that for vertical measurement, two-button BPMs located at the top ($\pi/2$) and bottom ($-\pi/2$) in Fig. 3(a) would have some advantages compared with Fig. 4. Plots of V_{px}/V_{ps} for θ_o from $-\pi/2$ to $+\pi/2$ give the same results as Fig. 4.

5 INVERTED BPM COEFFICIENTS

For the measurements of beam positions, x_o and y_o must be expressed in terms of $V_x = V_{px}/V_{ps}$ and $V_y = V_{py}/V_{ps}$. For the optimized configuration in a small-gap ($h = 2.0$ mm, $x_1 = 0$, and $x_2 = 4.0$ mm), as an example, the inverted polynomial coefficients for the BPMs were calculated from Eqs. (6), (7), and $V_{px}(x_o, y_o)$ as

$$x_o = (1.960 - 2.850V_y^2)V_x + (1.684 + 1.057V_y^2)V_x^3,$$

$$y_o = (1.902 - 0.162V_x^2)V_y + (0.120 + 0.178V_x^2)V_y^3, \quad (9)$$

for the region $|x_o| < 2$ mm and $|y_o| < 1.5$ mm. As Fig. 2(a) predicts, the coefficients for y_o were not changed for different regions and were relatively small, except for the first one.

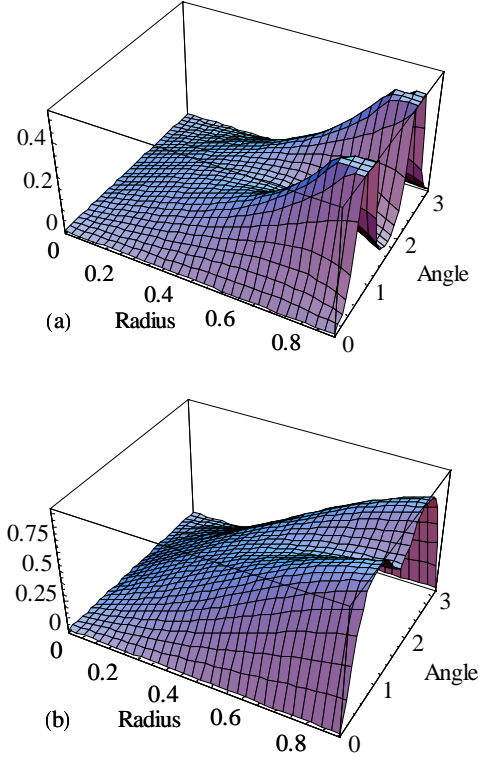


Figure 4: 3-D plot of (a) V_{py} and (b) V_{py}/V_{ps} calculations for four-button BPMs in the circular beam chamber with parameters of $\theta_p = \pi/4$ and $\Delta\theta = 0.5236$ rad.

6 CONCLUSIONS

Green's reciprocity relation for electrostatic problems was applied to calculate four-button BPM coefficients in simple chamber geometries. It was shown that finding induced charges on the buttons due to a charge at a beam position is equivalent to finding induced potential at a beam position due to given potentials on the buttons. In the case of finite-element modeling, only one set of mesh geometry is sufficient for the calculations.

7 REFERENCES

- [1] D.A. Goldberg and G.R. Lambertson, "A Primer on Pickups and Kickers," in *Physics of Particle Accelerators*, eds. M. Month and M. Dienes, AIP Conf. Proc. 249, p. 537 (1992).
- [2] S.H. Kim, "Optimization of Four - Button BPM Configuration for Small-Gap Beam Chambers," in *Beam Instrumentation Workshop*, eds. R.O. Hettel, S.R. Smith and J.D. Masek, AIP Conf. Proc. 451, p. 310 (1998).